Biomed Microdevices (2007) 9:911–922
DOI 10.1007/s10544-006-9040-4

Design and fabrication of an artificial cornea based on a photolithographically patterned hydrogel construct

David Myung · Wongun Koh · Amit Bakri · Fan Zhang · Amanda Marshall · Jungmin Ko · Jaan Noolandi · Michael Carrasco · Jennifer R. Cochran · Curtis W. Frank · Christopher N. Ta

Published online: 20 January 2007

Abstract We describe the design and fabrication of an artificial cornea based on a photolithographically patterned hydrogel construct, and demonstrate the adhesion of corneal epithelial and fibroblast cells to its central and peripheral components, respectively. The design consists of a central "core" optical component and a peripheral tissue-integrable "skirt." The core is composed of a poly(ethylene glycol)/poly(acrylic acid) (PEG/PAA) double-network with high strength, high water content, and collagen type I tethered to its surface. Interpenetrating the periphery of the core is a microperforated, but resilient poly(hydroxyethyl acrylate) (PHEA) hydrogel skirt that is also surface-modified with collagen type I. The well-defined microperforations in the peripheral component were created by photolithography using a mask with radially arranged chrome discs. Surface modification of both the core and skirt elements was accomplished through the use of a photoreactive, heterobifunctional crosslinker. Primary corneal epithelial cells were cultured onto modified and unmodified PEG/PAA hydrogels to evaluate whether the central optic material could support epithelialization. Primary corneal fibroblasts were seeded onto the PHEA hydrogels to evaluate whether the peripheral skirt material could support the adhesion of corneal stromal cells. Cell growth in both cases was shown to be contingent on the covalent tethering of collagen. Successful demonstration of cell growth on the two engineered components was followed by fabrication of core-skirt constructs in which the central optic and peripheral skirt were synthesized in sequence and joined by an interpenetrating diffusion zone.

Keywords Artificial cornea · Keratoprosthesis · Photolithography · Tissue integration · Epithelialization · Double-network · Interpenetrating network · Hydrogel

D. Myung · A. Bakri · J. Noolandi · C. N. Ta
Department of Ophthalmology, Stanford University School of Medicine,
300 Pasteur Drive, Stanford, CA 94305-5080, USA

D. Myung · A. Marshall · J. Ko · J. Noolandi · C. W. Frank
Department of Chemical Engineering, Stanford University,
381 North-South Mall, Stauffer III, Stanford, CA 94305, USA

W. Koh
Department of Chemical Engineering, Yonsei University,
134 Shinchon-dong, Seodaemoon-ku, Seoul 120-749, South Korea

F. Zhang · J. R. Cochran
Department of Bioengineering, Stanford University,
318 Campus Drive, Clark Center, Stanford, CA 94305, USA

M. Carrasco
Department of Chemistry, Santa Clara University,
500 El Camino Real, Santa Clara, California 95053, USA

C. N. Ta (✉)
Department of Ophthalmology, Stanford University,
900 Blake Wilbur Drive, W3036, Stanford, CA 94304-5353, USA
e-mail: cta@stanford.edu

1 Introduction

Artificial corneas (keratoprostheses) have potential to benefit millions worldwide who are blind due to corneal disease. However, the fabrication of synthetic stromal equivalents with the long-term transparency, biomechanical properties, and regenerative capacity of a human donor cornea remains a formidable challenge. This work presents the design, development, and preliminary evaluation of a photolithographically fabricated, photochemically surface-modified construct that builds upon the design of current corneal prostheses. Our approach consists of a poly(ethylene glycol)/

poly(acrylic acid) (PEG/PAA) double-network "core" optic component that supports surface epithelialization and an interpenetrating, microperforated poly(hydroxyethyl acrylate) (PHEA) "skirt" that promotes stromal tissue integration.

This design strategy is attractive for the following reasons. First, double-network hydrogels are distinguished from conventional single network hydrogels by their extremely high mechanical strength despite high levels of water (> 70%) (Gong et al., 2003). Second, a mechanically enhanced PEG/PAA double-network is a particularly advantageous combination for an optical device due to the hydrophilicity, mutual miscibility, and high protein-resistivity of PEG and PAA (Cruise et al., 1998; Czeslik et al., 2004; Myung et al., 2005; Olabisi et al., 1979; Padmavathi and Chatterji, 1996; Wittemann et al., 2003). Third, PHEA is a hydrophilic, cytocompatible, and rapidly photopolymerizing network that can readily interpenetrate with PEG and PAA and be patterned with high fidelity due to a low degree of swelling after polymerization (Gao et al., 2003; Guan et al., 2000; Moser et al., 1992). Fourth, the application of photolithographic patterning provides both spatial and temporal control over the conversion of a liquid monomer solution into a gel, allowing complex shapes to be fabricated (Albrecht et al., 2005; Liu and Bhatia, 2002; Nguyen and West, 2002; Tsang and Bhatia, 2004). Finally, photochemical surface modification can be used with micron-order precision to promote site-specific epithelialization and bulk tissue integration in otherwise protein-resistant hydrogels (Matsuda et al., 1990; Matsuda and Sugawara, 1995; Nakayama and Matsuda, 1999).

Our approach builds upon the pioneering work of other investigators who, through clinical evaluation of their devices, have identified the material properties necessary for improved retention and functionality *in vivo*. Arguably, the standard has been set by the Boston keratoprosthesis developed by Dohlman and colleagues, which is a core-and-skirt construct comprised of poly(methyl methacrylate) (PMMA), a transparent, biocompatible plastic. This device is successful in restoring visual acuity and can persist in a patient's eye for years (Doane et al., 1996). With the recent availability of softer, more hydrophilic materials, the approach toward synthetic cornea design has rapidly evolved from solely ocular, rigid prostheses to hydrated matrices designed for the regeneration of host tissue (Carlsson et al., 2003). As a result, artificial cornea research and development worldwide has shifted focus to soft and wet materials including hydrogels and biopolymeric scaffolds.

The most successful example of a hydrogel-based synthetic cornea is the AlphaCor keratoprosthesis, a poly(hydroxyethyl methacrylate) (PHEMA) copolymer developed by Chirila, Hicks, and coworkers (Chirila, 2001; Hicks et al., 1996, 1997a, b, 1998). The central optic component of AlphaCor is a homogeneous PHEMA network with good mechanical strength. However, this material only has a maximum achievable water content of 40%; at higher percentages, PHEMA phase separates to form a porous, opaque, but fragile "sponge" (Lou and Coppenhagen 2001). This sponge is the primary component of the peripheral skirt which promotes fibroblast integration. AlphaCor reportedly has a 1-year retention rate of about 80%, (Hicks et al., 2003).

While the advent of the Boston and AlphaCor keratoprostheses, as well as other innovative prosthetic designs (Cardona, 1991; Hille et al., 2002; Pintucci et al., 1996; Strampelli, 1972; Tsuk et al., 1997), represent significant milestones toward the development of a more biomimetic artificial cornea, their shortcomings have highlighted design parameters that need to be addressed for the long-term safety and stability of these devices. In general, a number of complications have limited their widespread applicability. These complications include retroprosthetic membrane formation, calcification, rejection, extrusion, infection (endophthalmitis), and glaucoma (Aquavella et al., 1982; Barber 1988; Hicks et al., 1997a; Nouri et al., 2001; Vijayasekaran et al., 2000). In most cases, these complications can be attributed to the device's material properties. For instance, protein adsorption has been postulated to be the molecular event that triggers calcification, inflammation, and retroprosthetic membrane formation that lead to visual loss in corneal prosthetics (Vijayasekaran et al., 2000). Low permeability to nutrients precludes the regrowth of the epithelium, which serves as a barrier to contamination by microbials or particulates. High rigidity in a material, in addition to making a keratoprosthesis vulnerable to extrusion, is implicated in the development of glaucoma (Khan et al., 2001; Carlsson et al., 2003). These events are directly related to the intrinsic properties of the implant material and represent the major limitations of current corneal prostheses. As a result, artificial corneas are almost always reserved for cases where transplantation of human donor tissue fails.

Griffith and co-workers have made significant progress toward a more biointegrable artificial cornea. They have recently reported particularly impressive *in vivo* results with a copolymeric extracellular matrix replacement based on collagen, poly(N-isopropylacrylamide) (NIPAAm), and N-acryloxysuccinimide. In porcine models, this material fosters epithelial, stromal, and nerve regeneration, and is currently undergoing clinical trials for therapeutic use in humans (Li et al., 2003).

The aforementioned efforts have identified critical design parameters for a more successful artificial cornea. The optimal corneal replacement would be mechanically strong, optically clear, capable of robust integration with surrounding ocular tissue, permeable to nutrients, and supportive of surface epithelialization (Chirila, 2001). Moreover, it would be resistant to protein adsorption to prevent complications leading to opacification and visual loss.

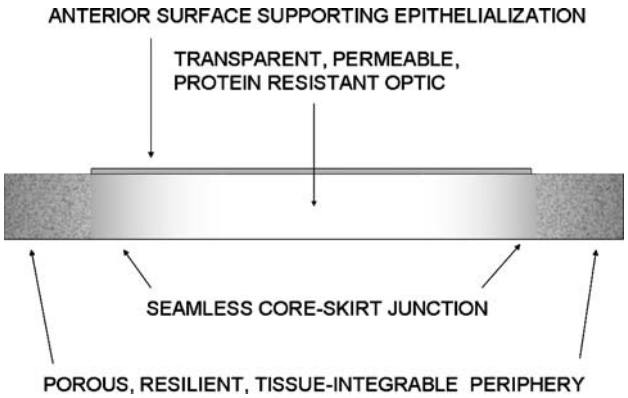

Fig. 1 Schematic of the ideal artificial cornea highlighting the critical design parameters for long-term *in vivo* success

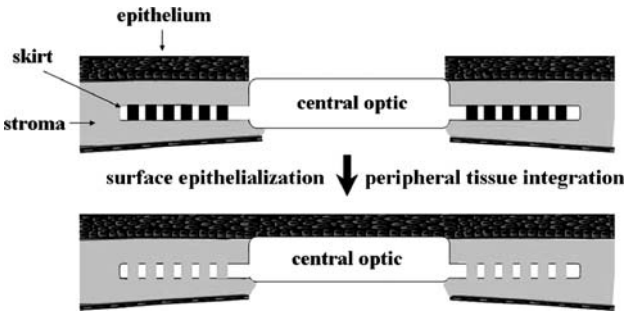

Fig. 2 Idealized schematic of how the proposed device prototype would function when implanted in a cornea *in vivo*. The peripheral skirt would be sandwiched between layers of the corneal stroma. Implantation is followed by surface epithelialization and tissue integration within the peripheral pores

We hypothesized that intrinsically protein-resistant, mechanically enhanced polymers that are engineered for site-specific cell growth would provide the basis for a more sustainable artificial cornea. Figure 1 shows the schematic inspired by these design parameters that served as the blueprint for the construct presented in this paper. It features: (1) a transparent central optic that is both permeable to glucose and resistant to the adsorption of proteins, (2) a bioactive anterior surface that supports the adhesion and growth of epithelial cells, (3) a porous, yet resilient periphery designed to encourage the ingrowth of fibroblasts, and (4) a seamless junction between the core and the skirt. Accomplishment of these engineering parameters in a single keratoprosthetic construct is anticipated to enhance its probability of long-term retention. The idealized schematic in Fig. 2 depicts how the proposed device (with modifications to the central and peripheral thicknesses) would function when implanted in a living cornea. The peripheral rim of the device would be "tucked" between dissected layers of the corneal stroma. This keratoprosthesis is designed to encourage epithelialization on its surface and fibroblast ingrowth within the peripheral pores to anchor it to the surrounding stroma.

2 Materials and methods

2.1 Central optic hydrogel synthesis

PEG/PAA hydrogels were synthesized by a two-step sequential network formation technique based on UV-initiated free radical polymerization. A precursor solution for the first network was made of purified PEG-diacrylate (MW 8000) (Quinn et al., 1995) dissolved in deionized water with 2-hydroxy-2-methyl propiophenone as the UV-sensitive free radical initiator. The solution was cast into a glass/Teflon mold, covered with a glass plate, and reacted under a Xenon UV light source (1 mW/cm^2, Oriel Instruments) at room temperature. Upon exposure, the precursor solution underwent a free-radical-induced gelation and became insoluble in water. To incorporate the second network, the PEG hydrogel was removed from the mold and immersed in a 50% v/v acrylic acid solution with 1% v/v with respect to the monomer hydroxyl-2-methyl propiophenone as the photoinitiator, and 1% v/v with respect to the monomer triethylene glycol dimethacrylate as the cross-linking agent for 24 h at room temperature. The swollen gel was exposed to the UV source and the second network was polymerized inside the first network to form a double-network structure. Following synthesis, the hydrogels were washed extensively for 5 days in Dulbecco's phosphate buffered saline (DPBS) with repeated solvent exchanges to remove any unreacted components.

2.2 Swelling measurements

The water content of the hydrogels was evaluated in terms of the swollen-weight-to-dry-weight ratio. The dry hydrogel was weighed and then immersed in water as well as Dulbecco's phosphate buffered saline. At regular intervals, the swollen gels were lifted, patted dry, and weighed until equilibrium was attained. The percentage of equilibrium water content (WC) was calculated from the swollen and dry weights of the hydrogel:

$$WC = \frac{W_S - W_d}{W_S} \times 100 \quad (1)$$

where W_S and W_d are the weights of swollen and dry hydrogel, respectively.

2.3 Optical properties

The refractive index of the PEG/PAA hydrogel (with PEG MW 8000) was measured using an Abbe Refractometer (Geneq, Inc., Montreal, Quebec). The percentage (%) of light transmittance of this hydrogel at 550 nm was also measured using a Varian Cary 1E/Cary 3E UV-Vis spectrophotometer following the method described by Saito et al. (2003).

2.4 Peripheral skirt fabrication

An aqueous solution of 2-hydroxyethyl acrylate (HEA), 1% v/v with respect to the monomer 2-hydroxy-2-methyl propiophenone (photoinitiator), and 1% v/v with respect to the monomer triethylene glycol dimethacrylate (Sigma) was prepared in deionized water. The solution concentration (v/v) of HEA was varied between 50% and 80% to determine synthesis conditions which yielded the best mechanical strength and patterning results. For mechanical measurements, PHEA hydrogels prepared from precursor solution concentrations ranging from 50% to 80% were synthesized as unpatterned homogeneous sheets. For skirt fabrication, the solutions were injected between a glass/chrome photomask (Advance Reproductions, Andover, MA) and another glass plate with an intervening Teflon spacer (250 μm thick) beneath the pattern of interest. The photomask consists of six different patterns with variations in the radius of the unpatterned region (r), and the number (n), diameter (D), spacing (L), and degree of radial separation (θ) as diagrammed in Fig. 3(a). These parameters were designed to yield hydrogels up to 500 μm thick with an unpatterned, transparent central region (of radius 1000 μm or 2000 μm) and a peripheral region with a radial array of pores of diameters of either 60 μm or 120 μm spaced 10–20 μm apart, along 1–2 degrees (θ) of radial separation. Photographs of the photomask pattern used in this study are shown in Figs. 3(b) and (c). Figure 3(b) shows a mask with discs of diameter 120 μm spaced 10 μm apart along 1 degree of radial separation. Figure 3(c) shows a magnified view of this pattern. Figure 3(d) shows a magnified view of a different pattern (not used) with the same disc spacings but with 60 μm pores. The disc diameters were chosen in order to produce pores within hydrogels that can accommodate multiple cells (roughly 10–15 μm diameter each) per horizontal cross-section and to allow room for extracellular matrix deposition. The radial pattern was chosen in anticipation that stress will be distributed in this way around the implant. Additional patterns have been fabricated consisting of grid patterns, but they were not used in this study. To synthesize the microperforated PHEA hydrogel, the aqueous monomer solution (80% v/v) was exposed to a UV light source for 60 s through the photomask. The resultant porous hydrogel was then washed extensively in water to remove the unreacted monomers that were directly beneath the chrome regions on the mask.

2.5 Mechanical testing

The PEG/PAA system with PEG MW 8000 was previously determined to have the optimum glucose permeability and was the primary focus of central optic mechanical testing (Bakri et al., 2006; Myung et al., 2005). PHEA hydrogels of varying water content were also tested. Prior to testing, the PEG, PAA, PEG/PAA, and PHEA hydrogels were swollen to equilibrium in Dulbecco's phosphate buffered saline (DPBS) overnight. The specimens were cut into rectangular strips (length 10.0 mm, width 3.0 mm, and thickness 250 μm–750 μm) using a parallel-blade cutting tool. PEG, PAA, PEG/PAA, and PHEA hydrogel specimens were tested using an Instron 5844 materials testing apparatus equipped with a 10 N load cell (Instron Corp., Norwood, MA) and were kept moist during testing with an ultrasonic humidifier. Hydrogel thickness was measured by gently clamping a digital caliper (VWR International, Westchester, PA) over samples sandwiched between 0.15 μm thick glass coverslips in order not to compress or damage the hydrogels. The

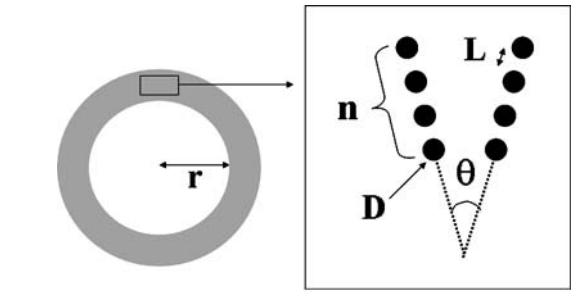

(a)

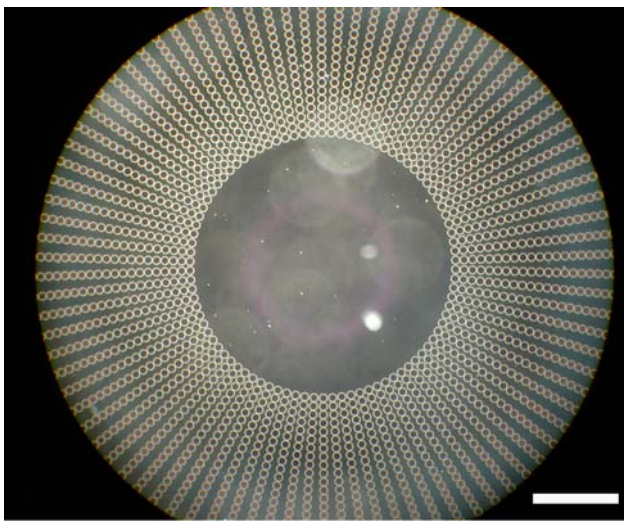

(b)

Fig. 3 (a) Schematic of photomask with chrome disc pattern parameters r = radius of unpatterned region in (μm), n = number of discs per radius, D = diameter of disc (μm), L = distance between disc edges (μm), and θ = degree (°) of separation between disc lines. (b) Photograph of a mask with the following chrome disc pattern parameters r = 2000 μm, n = 50, d = 120 μm, L = 10 μm, and θ = 1°. Scale bar = 1300 μm. (c–d) Magnifications of photolithographic patterns used to synthesize microchanneled hydrogel skirts. On the left is a radial pattern of chrome discs with 4 cm diameter unpatterned central region, 120 μm diameter discs spaced 10 μm apart along radial lines with 1° of separation.) On the right is a pattern with the same disc spacings but with 60 μm disc diameter. Scale bars = 120 μm each

(*Continue on next page*)

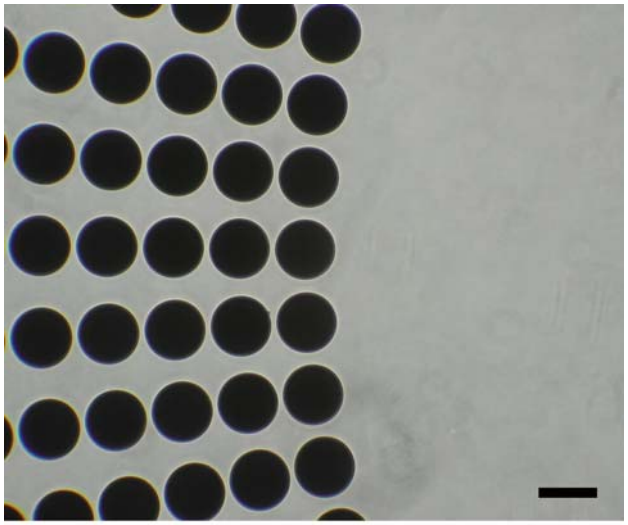

(c)

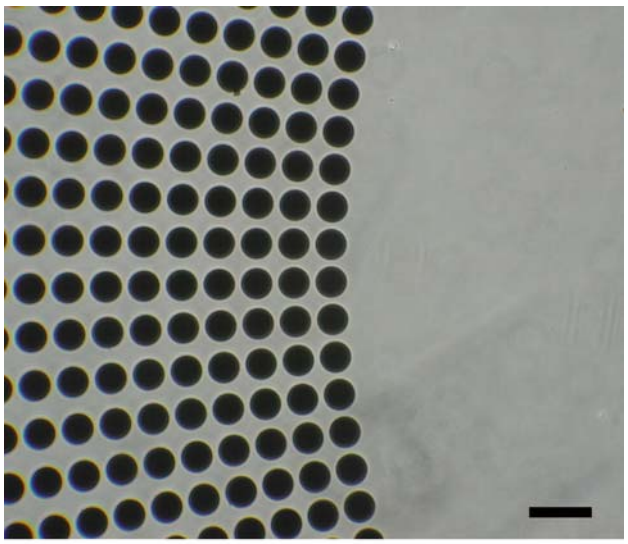

(d)

Fig. 3 (*Continued*)

crosshead speed was set at 15 mm/min for all samples. Load and extension measurements collected by Instron Bluehill software was then used to obtain the maximum true stress (tensile strength) of each sample.

2.6 Photochemical surface modification

Because the hydrogels used in this study exhibit high resistance to non-specific protein adsorption, their surfaces had to be photochemically modified to enable covalent linkages with proteins and to facilitate the adhesion of cells. To couple collagen type I to the hydrogel surfaces, the heterobifunctional crosslinker, 5-azidonitrobenzoyloxy N-hydroxysuccinimide (Fig. 4) was used, which has a phenyl azide group on one end and a protein-binding N-hydroxysuccinimide group on the other. Substituted

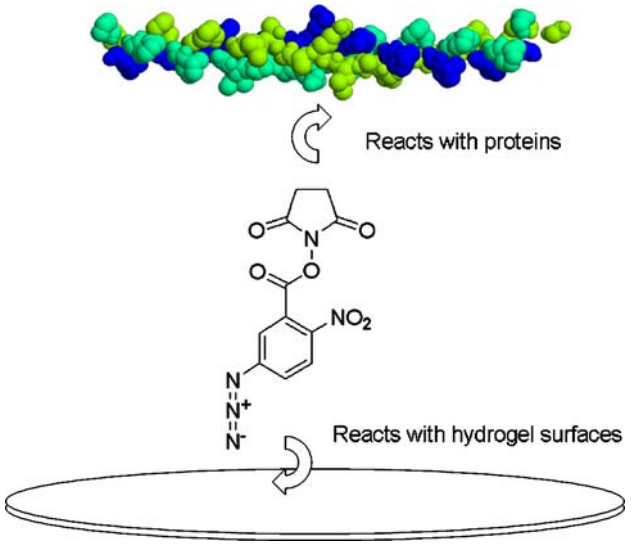

Fig. 4 The heterobifunctional crosslinker, 5-azidonitrobenzoyloxy N-hydroxysuccinimide (center), was used to covalently bind collagen type I to the surface of PEG/PAA and PHEA hydrogels. The phenyl azide group on end of the crosslinker (bottom) is activated by UV light and binds to the hydrogel surface, leaving the N-hydroxysuccinimide other end (top) free to react with free amines on proteins. (Source of crosslinker image: Sigma-Aldrich)

phenyl azides have been shown to react with light (250–320 nm, 5 min) to generate aromatic nitrenes, which insert into a variety of covalent bonds (Matsuda et al., 1990; Matsuda and Sugawara, 1995). Attachment of the linker to the hydrogel via the phenyl azide group then allows the *N*-hydroxysuccinimide groups to react with free amines on proteins, and in turn, tether them to the hydrogel surface.

The surfaces of the hydrogels were dabbed dry and then 100 μL of a 0.5% w/v solution of 5-azidonitrobenzoyloxy *N*-hydroxysuccinimide in dimethylformamide was drop-casted onto the gel and spread evenly over its surface. The solvent was then allowed to evaporate under a fume hood to ensure deposition of the crosslinker onto the hydrogel. The air-dried gel surface was then exposed to UV light for 5 min to react the azide groups to the hydrogel surface. The surface-functionalized gels were then incubated in a 0.3% (w/v) collagen type I solution (Vitrogen) in a 37°C oven for 16 h to couple reactive protein amine groups to the *N*-hydroxysuccinimide moieties on the hydrogel surface. Finally, the gels were washed extensively in DPBS to remove organic solvent and unreacted monomers. The presence of tethered protein on the surface was confirmed by X-ray photoelectron spectroscopy.

2.7 Primary corneal epithelial cell culture

Primary corneal epithelial cells were isolated from rabbit corneas by an explant method described by Trinkaus-Randall

et al. (1990b). Corneas were aseptically removed from rabbit eyes and immersed in an antibiotic/phosphate buffered saline solution, then immersed in 1.2 U/ml Dispase II in Dulbecco's modified eagle medium (DMEM) for 1 h. Sheets of epithelium were removed from the corneal surface and placed in tissue culture dishes containing DMEM fortified with 0.5% premixed insulin-transferrin-selenium (Becton-Dickinson), 5% fetal bovine serum, and 1% penicillin/streptomycin. Cells were cultured for an additional 10 days, with media changes every 2–3 days (Griffith et al., 2002). The cells were then seeded at a concentration of 1×10^5 cells/mL onto unmodified PEG/PAA hydrogels and PEG/PAA hydrogels with photochemically bound collagen type I on its surface.

2.8 Primary corneal fibroblast cell culture

Corneas were excised from rabbit eyes obtained from Pelfreez Biologicals (Rogers, Arkansas). Fibroblasts were cultured from the corneas in the following manner: Descemet's membrane and endothelium were removed with forceps, and the remaining epithelium and stroma were incubated in Dulbecco's Modified Eagle's Medium (DMEM) and 1.2 U/ml Dispase II for 1 h. Sheets of epithelium were removed from the basement membrane, and then the remaining stroma was minced and incubated for 1 h at 37°C in serum-free medium with 500 μg/ml bacterial collagenase Type IA (Sigma). After 1 h, the digested tissue was centrifuged at 800 g for 10 min, washed with DMEM with 10% fetal bovine serum, and centrifuged again. The pellet was resuspended with DMEM, 0.5% insulin-transferrin-selenium (Becton Dickinson), 10% fetal bovine serum, and seeded onto tissue culture flasks. After 7 days, the cells were subcultured for seeding onto substrates of interest (Trinkaus-Randall et al., 1990a). The cells were then seeded at a concentration of 1×10^5 cells/mL onto patterned PHEA hydrogels with and without photochemically coupled collagen type I on their surface.

2.9 Core-and-skirt prototype fabrication

To synthesize the skirt around the periphery of the central optic, the PHEA precursor solution was injected around a previously synthesized central optic disc centered over the unpatterned region of the mask. The HEA monomer was allowed to diffuse into the periphery of the optic for 30 minutes, and then the photomask was placed under a UV light source for 60 s. The resulting core-skirt construct was then removed from the plates, washed extensively in water, and then stored in DPBS until further use.

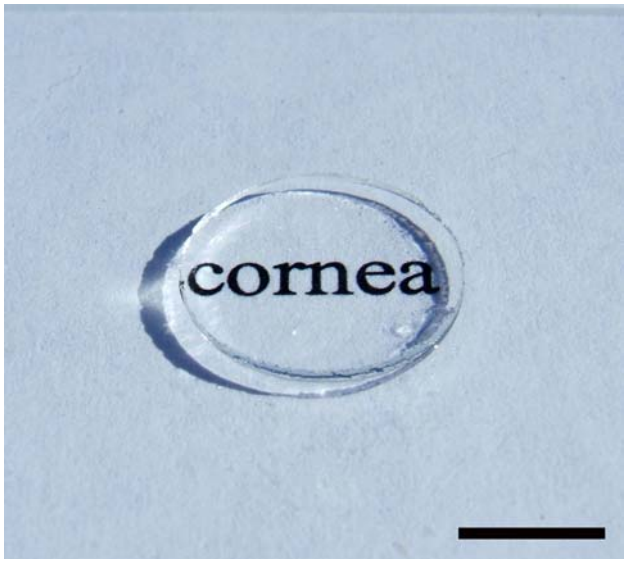

Fig. 5 A PEG/PAA hydrogel designed for use as a central optic component of an artificial cornea. The hydrogel contains 85% water, has high tensile strength (1.1 MPa) and light transmissibility (96%), and a refractive index of 1.35. Scale bar = 6.0 mm

3 Results

3.1 Hydrogel synthesis and physical characterization

Hydrogel synthesis yielded central optics with excellent mechanical and optical properties. Figure 5 demonstrates the optical clarity of the saline-swollen PEG/PAA hydrogel, which is on a glass plate overlying printed text. This material is highly transparent (96% light transmissibility) and has a refractive index of 1.35, slightly less than that of the natural cornea (1.376) (Ismail, 2002). Despite having high water content (85%), PEG/PAA has high tensile strength (1.1 MPa). The physical properties of the PEG/PAA hydrogel are summarized in Table 1.

Normal physiologic intraocular pressure (IOP) ranges from 10 to 21 mm Hg. In the event of acute-angle glaucoma, the IOP may reach 70 mm Hg in a severe case. *In vivo* studies on rabbits have shown that IOP is elevated to about ten times that of normal when the eye is manually massaged. At an IOP of 180 mm Hg, however, the ocular blood supply is cut off. Based on these scenarios, Nash et al. determined that the very upper limit of stress that a typical cornea may encounter is no more than 268 mm Hg, which correlates with

Table 1 PEG/PAA central optic hydrogel properties

Property	Measured value
Water content	85%
Tensile strength	1.1 MPa
Transparency	96%
Refractive index	1.35

Table 2 PHEA hydrogel properties

Monomer concentration (v/v)	Final hydrogel water content (w/w)	Tensile strength
50%	74%	170 kPa
60%	66%	210 kPa
80%	62%	470 kPa

a uniaxial tensile stress of approximately 250 kPa. At levels higher than this, physiologic relevance is lost (Hoeltzel et al., 1992; Nash et al., 1982). Therefore, a threshold of 250 kPa was used as the criterion for adequate mechanical strength in the PHEA hydrogels.

PHEA hydrogels with varying water content were prepared from different HEA monomer solution concentrations. Uniaxial tensile tests revealed that the PHEA hydrogel containing 62% water (prepared from an initial monomer concentration of 80%) had the best mechanical properties, with tensile strength of 470 kPa. The PHEA gels containing 66% and 74% water had inferior properties, with tensile strength values of $\leq$210 kPa. These results are summarized in Table 2. Based on our criteria of 250 kPa as the minimum tensile strength to resist intraocular pressure fluctuations *in vivo* (Nash et al., 1982), we settled on the PHEA network containing 62% water for subsequent patterning experiments.

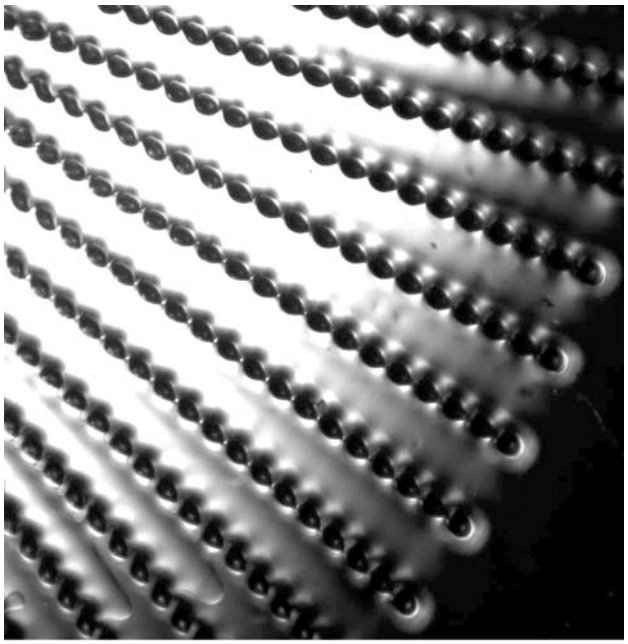

(a)

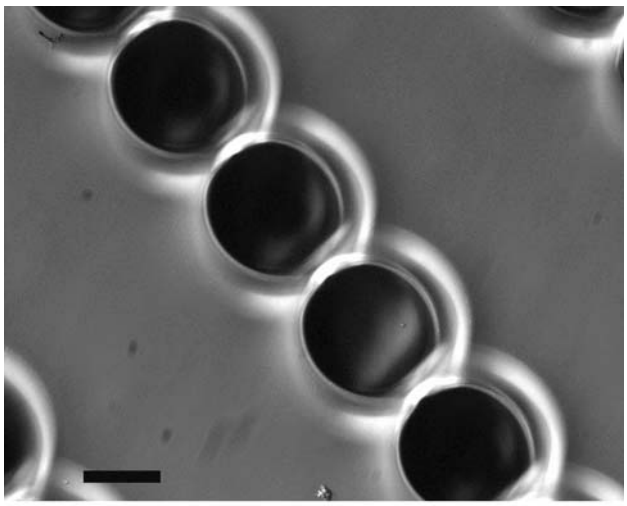

(b)

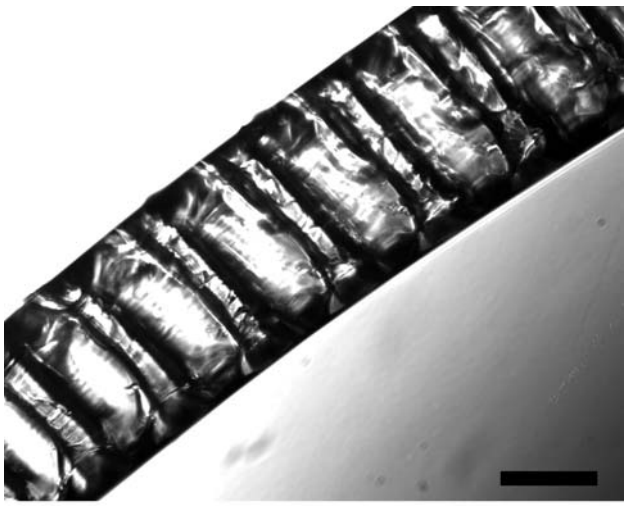

(c)

Fig. 6 (a) Photograph (top view) of a photolithographically patterned PHEA hydrogel fabricated using the photomask shown in Figs. 3(b) and (c). (b) Magnified view of the photolithographically patterned PHEA hydrogel shown in Fig. 6(a). Scale Bar = 100 μm. (c) Photograph of a cross-section through the pores of the patterned PHEA hydrogel in Figs. 6(a) and (b). The pores pass all the way through the hydrogel (250 μm thick), and are designed to be avenues for cellular ingrowth. Scale bar = 100 μm

Fig. 6 (*Continued*)

Photolithographic patterning of the 80% (v/v) HEA precursor solution yielded hydrogels furnished with regular, radial arrays of pores. Figures 6(a) and (b) shows that the patterning process successfully produced the desired radial porous array despite some swelling after polymerization (the pore diameter increased about 50%). The cross-section shown in Fig. 6(c) demonstrates that the photolithographic process yields pores that go completely through the gel to provide avenues for stromal tissue integration as illustrated previously in Fig. 2.

3.2 Surface modification and characterization

To confirm the tethering of collagen type I to the hydrogels, we employed X-ray photoelectron spectroscopy (XPS) to

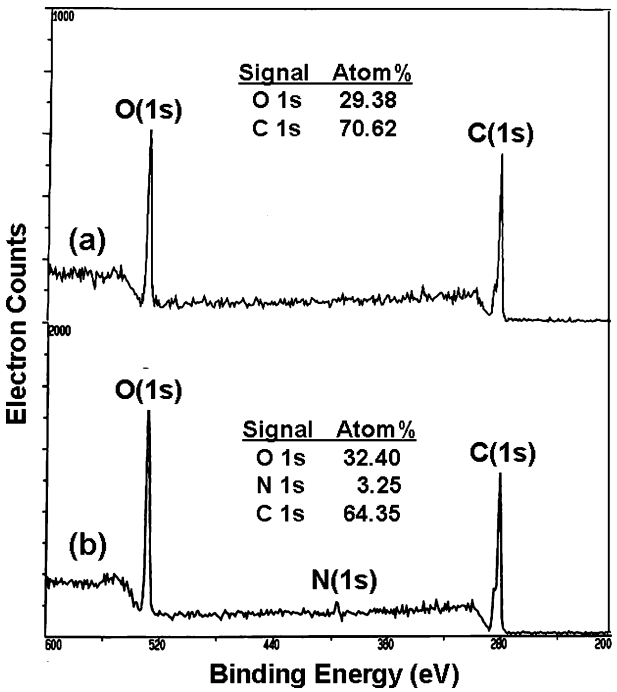

Fig. 7 XPS spectrum of a PEG/PAA hydrogel surface-modified with collagen type I by azide active-ester linkage (lower spectrum), compared with an unmodified PEG/PAA hydrogel surface (upper spectrum). The appearance of the nitrogen peak is indicative of the presence of amide linkages between collagen and the hydrogel surface

confirm the presence of peptide linkages on both unmodified and modified hydrogels (Fig. 7). In the absence of surface modification, only oxygen and carbon peaks are present in the spectrum, corresponding to the unmodified hydrogel surface. In the spectrum of the collagen-tethered hydrogel, there is an additional peak corresponding to the presence of nitrogen atoms due to amide linkages between collagen and the hydrogel surface.

3.3 Corneal epithelial and fibroblast growth on hydrogels

Primary rabbit corneal epithelial cells were able to adhere and grow to confluence on surface-modified PEG/PAA double-network hydrogels. Early passage rabbit corneal epithelial cells were seeded on substrates at a concentration of 1.0×10^5 cells/cm^2. The epithelial cells exhibited excellent spreading ($> 75\%$) on collagen-bound PEG/PAA networks within 2 h, achieved confluency within 48 h, and had migrated over the remainder of the unseeded surface by day 5. A representative photomicrograph of the adherent cells grown to confluence is shown in Fig. 8(a). In contrast, cells were not able to spread on unmodified PEG/PAA (not shown). Moreover, cell spreading was not observed when the PEG/PAA hydrogels were simply incubated with collagen type I (0.3%) without prior azide-active-ester functionalization, demonstrating that the intrinisic protein resistance of the PEG/PAA hydrogel prevents cellular adhesion to this material (Fig. 8(b)). It also confirms that the photochemical cross-linking strategy we employ is effective at producing robust bioactivity on an otherwise inert hydrogel surface. Primary rabbit corneal fibroblast cells were also able to adhere and grow to confluence on collagen type I-modified PHEA. Early passage rabbit corneal fibroblasts were seeded onto microperforated PHEA substrates at a concentration of 1.0×10^5 cells/cm^2. The cells reached confluence on the central, anterior surface of the section of the PHEA gel within 24 h (Fig. 8(c)).

3.4 Core-and-skirt prototype fabrication

Step-wise fabrication of core-and-skirt constructs was carried out first by synthesizing a PEG/PAA central optic and then interpenetrating its periphery with a photolithographically patterned PHEA skirt using the technique illustrated in Figs. 9(a–c). Fusion between the core and skirt was achieved by injecting the HEA monomer solution around the periphery of the central optic and allowing it to diffuse into it for 30 mins. Photolithographic patterning of the HEA precursor yielded a PHEA hydrogel that was integrated with the central optic and was porous below the masked regions where the HEA solution remained in liquid form and was subsequently washed away. This fabrication process yielded constructs with a PEG/PAA central optic and a peripheral, microperforated PHEA skirt that could be manipulated easily with forceps; an example of a core-and-skirt artificial cornea prototype is shown in Fig. 10.

4 Discussion

The current work is a novel approach toward the fabrication of a tissue-integrable artificial cornea. Photolithographic patterning techniques were adapted to create a three dimensional hydrogel construct consisting of a double-network central optic and microperforated peripheral skirt that is covalently modified on its surface with collagen-type I. *In vitro*, the optic and skirt components were shown to facilitate the adhesion of the specific cells types they were engineered to attract *in vivo*. Figure 2 depicts how this device design would be expected to function in a living cornea. The peripheral skirt

Fig. 8 (a) Corneal epithelial cells grown to confluence on PEG/PAA ▶ with collagen type I coupled to its surface via azide-active-ester linkage. Scale bar = 50 μm. (b) Corneal epithelial cells seeded PEG/PAA hydrogel incubated in collagen type I without prior azide-active-ester functionalization. The lack of chemical bonding of collagen to the highly protein-resistant hydrogel prevents the adhesion and spreading of the cells. Scale bar = 50 μm. (c) Photomicrograph of corneal fibroblasts grown to confluence on PHEA with collagen type I coupled to its surface via azide-active-ester linkage. Scale bar = 100 μm

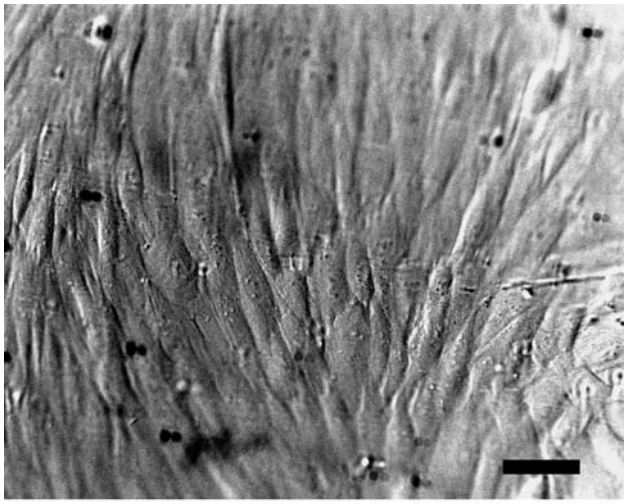

(a)

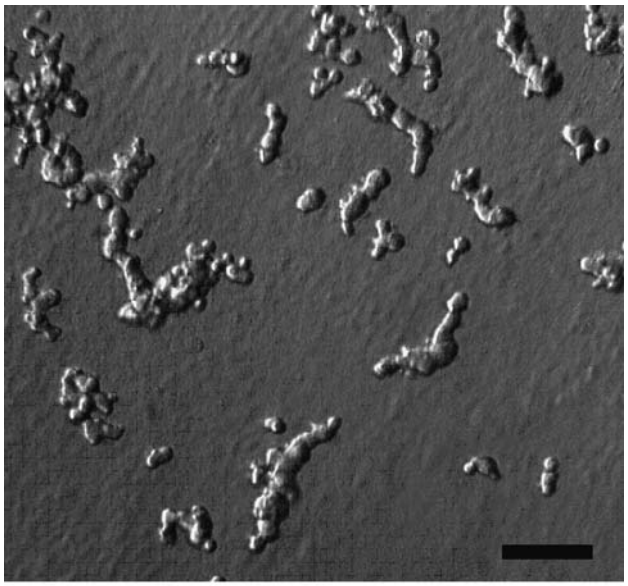

(b)

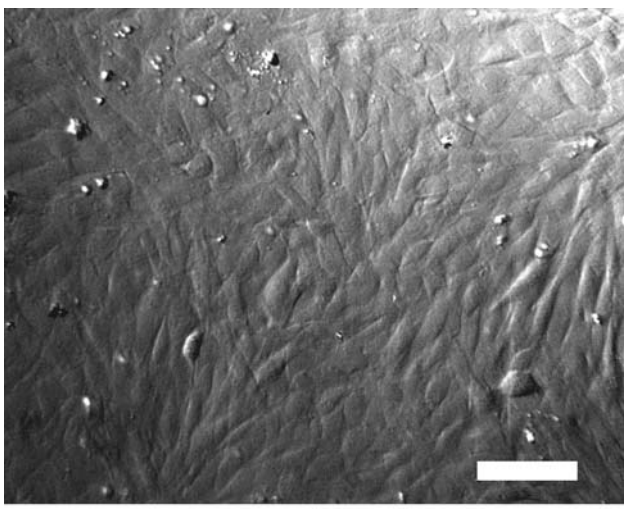

(c)

Fig. 8

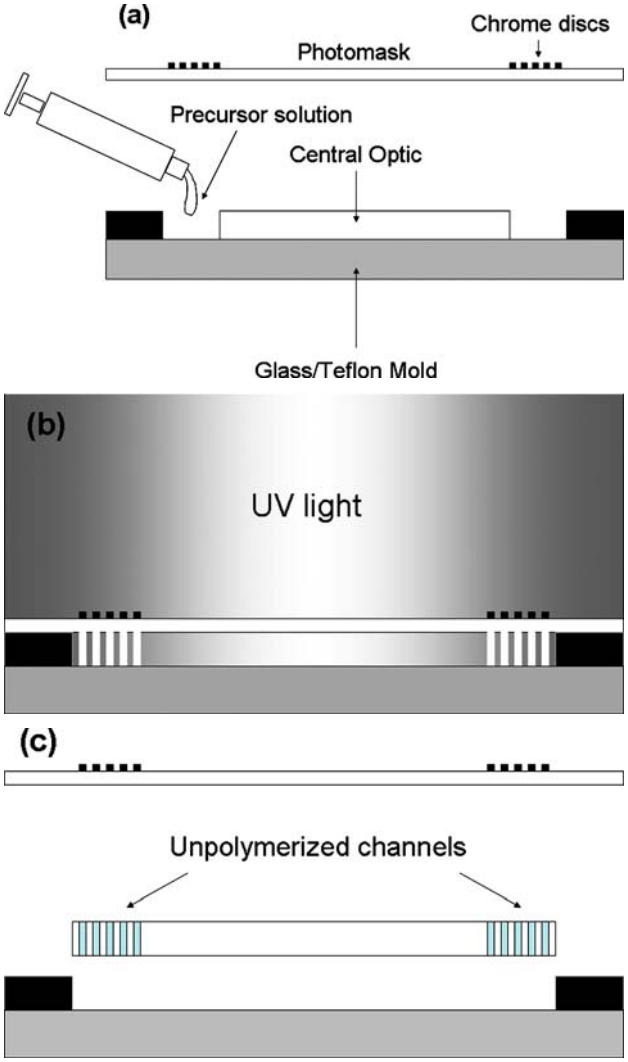

Fig. 9 (a–c) Photolithographic fabrication of the core-and-skirt keratoprosthesis is accomplished by (a) positioning a previously synthesized PEG/PAA central optic beneath the unpatterned region of a photomask and injecting the PHEA precursor solution around it. This is followed by (b) exposure to UV light through the mask. The resultant hydrogel construct (c) has vertical channels in its periphery because the solution directly under the chrome discs is not exposed to the UV light, and remains unpolymerized

would be implanted between layers of the stroma and sutured in place. Surgery would be followed by epithelial cell growth on the implant surface and stromal fibroblast ingrowth into the peripheral, microperforated skirt.

A prime obstacle in the development of biomimetic artificial corneas has been the interdependence of the four polymer material properties critical to their success: (1) optical clarity, (2) mechanical strength, (3) nutrient permeability (via high water content), and (4) capacity for biointegration. For example, an increase in mechanical strength usually entails the inclusion of tougher, but more hydrophobic polymers. However, increasing the hydrophobicity of the material tends to decrease its water content and permeability, which in turn

Fig. 10 A photolithographically patterned artificial cornea prototype with central optic and peripheral skirt. The central optic is composed of a PEG/PAA double-network hydrogel, which is interpenetrated in its periphery with a microperforated PHEA hydrogel skirt

has a negative effect on its ability to sustain epithelial cell growth, even in the presence of a bioactive surface. In the reverse scenario, increasing the permeability of a strong material requires increasing its water content or porosity. Unfortunately, increasing water content to the necessary level ($\sim$78%) by the inclusion of more hydrophilic species tends to compromise mechanical strength. Increasing porosity in the core component may negatively affect optical properties due to light scattering or unwanted tissue ingrowth centrally. This engineering "domino effect" makes removal of one deficiency in a candidate polymer difficult to accomplish without negatively affecting its other favorable properties. It is also the reason that mechanical enhancement of PEG by inclusion of another highly hydrophilic– and mutually miscible–polymer (PAA) is particularly advantageous, because the transparency and high water content are preserved.

From a biocompatibility and tissue integration standpoint, the high hydrophilicity of the PEG/PAA system has both advantages and disadvantages. The main advantage is high resistance to protein adsorption. Indeed, PEG and PAA are among the most effective polymers available for this purpose under physiologic conditions (Halperin, 1999; Wittemann et al., 2003). Preventing non-specific protein adsorption increases long-term biocompatibility and transparency. Preliminary work in our laboratory has shown that PEG/PAA hydrogels remain transparent in live rabbit corneas for periods of up to 6 weeks (Bakri et al., 2006). However, further *in vitro* and *in vivo* evaluation of the protein resistance of the PEG/PAA double-network combination is merited.

Although high protein resistance prevents unwanted nonspecific adsorption to a material, it also means that an additional surface modification strategy is required to facilitate cellular adhesion. Promotion of cell adhesion to polymers is most often accomplished by the incorporation of bioactive peptides and proteins through covalent immobilization. The extracellular matrix proteins collagen, fibronectin, and laminin as well as their peptide derivatives such as RGD and YIGSR, have been incorporated into various artificial cornea constructs to mimic the basement membrane of the natural corneal epithelium (Aucoin et al., 2002; Sweeney et al., 2003). While many hydrogel modification strategies involve the incorporation of adhesion-promoting ligands during polymerization, these do not allow for high concentrations of proteins at the tissue-implant interface because a large proportion of the ligands are inside the polymer and inaccessible to cells. Many current covalent coupling methods use condensation reactions at water-polymer interfaces. In these cases, active functional groups such as amino, carboxyl, hydroxyl, or mercapto groups must be present on polymer surfaces to form chemical bonds with proteins. However, chemical fixation with regional precision is difficult with these methods (Matsuda et al., 1990; Matsuda and Sugawara, 1995).

The use of photochemical patterning methods achieves this desired precision by allowing the localization of reactive groups on the surface of a polymer, and in turn facilitates the formation of a concentrated layer that acts like a basement membrane for attaching cells. Using photoreactive, azide-active-ester linkages developed by Matsuda and coworkers (Matsuda et al., 1990; Matsuda and Sugawara, 1995), we have covalently tethered collagen type I to the surfaces of PEG/PAA and PHEA hydrogels to promote corneal cell adhesion growth on these materials. This modification strategy was especially critical in the case of PEG/PAA due to their high protein resistance, since our experiments showed that simply trying to adsorb collagen to the hydrogels is ineffective at promoting epithelial cell adhesion (Fig. 8(b)). Collagen type I is the predominant extracellular matrix protein in the cornea and is suitable for therapeutic use in humans. Our results indicate that surface-tethered collagen type I provides a suitable matrix for the adhesion and growth of corneal epithelial cells and fibroblasts on PEG/PAA and PHEA, respectively. Future work includes, but is not limited to, evaluation of the barrier function and long-term integrity of the epithelium, as well as histological and immunohistochemical evaluation of the fibroblast ingrowth into the hydrogel skirts. It also entails continued optimization of the biointerface, with the goal of achieving robust and efficient epithelialization and tissue integration while maintaining normal differentiation of the migrating cells. For *in vivo* success, a rapid rate of tissue integration and epithelialization is important for anchorage of the device as well as the prevention of microbial contamination post-operatively.

Peripheral interpenetration of the central PEG/PAA optic with PHEA accomplishes three important goals: (1) high water content ($\geq 78\%$) in the optic, (2) controlled porosity in the periphery, and (3) a seamless junction between the two components. While it would be ideal if the core and skirt were comprised of the same material (either PEG/PAA or PHEA), this is a challenging problem for a number of reasons. PEG and PAA networks swell substantially after polymerization, which means that after photolithographic patterning, the original pore sizes and distributions are undesirably altered. When these polymers are prepared in sequence as an interpenetrating network, there are two rounds of swelling that affect the pores and diameter of the final device. This is the primary reason that PHEA, rather than PEG and PAA, was chosen as the skirt material for the first generation prototype. Not only does it rapidly polymerize (~ 1 min), but it exhibits a relatively mild degree of swelling after polymerization. Moreover, the rate of polymerization of acrylate monomers (such as 2-hydroxyethyl acrylate), in our experience (data not shown), is nearly an order of magnitude faster than that of methacrylate monomers (such as 2-hydroxyethyl methacrylate, the precursor of PHEMA). While methacrylate-based hydrogels would likely yield a stronger peripheral skirt, in our experience, its slow gelation makes it unsuitable for our patterning purposes. With longer UV exposure times, the masked regions tend to polymerize and the channels are effectively "filled in" with hydrogel material. Therefore, the choice of PHEA in the skirt represents the balance between good mechanical properties and polymerization rate. On the other hand, PHEA is unsuitable for use as the primary central optic material, since it attains the necessary tensile strength (> 250 kPa) only after its water content is reduced to 62%, which is insufficient for nutrient transport in the cornea.

Before the prototype presented in this paper is suitable for testing *in vivo*, however, a number of additional engineering parameters must be addressed. While the central optic has excellent optical, mechanical, and transport properties, it still falls short of the natural cornea, which has a refractive index of 1.376 and tensile strength on the order of several megapascals. The properties of the optic developed in this work have been demonstrated to be suitable for surgical implantation and ocular tolerance *in vivo* (Bakri et al., 2006). However, it is likely that continued optimization of the central optic material will be necessary to better approximate the natural cornea's properties in order to provide the best visual outcomes and avoid post-operative complications.

While the core-and-skirt constructs we have developed have good tensile strength and can easily be manipulated with forceps, the presence of peripheral pores still makes it vulnerable to fracture after implantation. Therefore, there is still room to improve the mechanical properties of the skirt, which ideally would have tensile strength and an elastic modulus on the order of megapascals. Optimization of the peripheral skirt will therefore require attention to the pore size and distribution that maximizes tensile strength under biaxial loading. Photolithography is not only an effective method to fabricate our device, but is also applicable as a high-throughput vehicle for determining the pore size and distribution that provides the best combination of mechanical strength and tissue integrability. Improvement of the bulk mechanical properties of the skirt through evaluation of various pore configurations as well as new (or modified) candidate materials is the subject of ongoing investigation.

5 Conclusions

A novel approach toward the fabrication of a tissue-integrable artificial cornea was presented. Photolithographic patterning techniques were adapted to create a three dimensional hydrogel construct consisting of a mechanically strong central optic with high water content and a resilient, microperforated peripheral skirt. The surfaces of the construct components were covalently modified with collagen-type I. *In vitro*, the optic and skirt were separately shown to facilitate the adhesion of the specific cells types they were engineered to attract in a living cornea. These results provide the foundation for future optimization of this prototype for subsequent implantation *in vivo*.

Acknowledgments This research was supported by the Bio-X Program and the Office of Technology Licensing at Stanford University. Instrument support was provided by the shared facilities at the Center on Polymer Interfaces and Macromolecular Assemblies (CPIMA) at Stanford University. The authors thank Stacey Bent and Jungsic Hong for use of the X-ray spectrometer and Beinn Muir for use of his high-resolution digital camera. Additional external support was also received from VISX, Incorporated (now VISX Technology) and the Fight for Sight Foundation.

References

D.R. Albrecht, V.L. Tsang, R.L. Sah, and S.N. Bhatia, Lab Chip **5**, 111–118 (2005).
J.V. Aquavella, G.N. Rao, A.C. Brown, and J.K. Harris, Ophthalmology **89**, 655–660 (1982).
L. Aucoin, C.M. Griffith, G. Pleizier, Y. Deslandes, and H. Sheardown, J. Biomater. Sci. Polym. Ed. **13**, 447–462 (2002).
A. Bakri, N. Farooqui, D. Myung, W.G. Koh, J. Noolandi, M. Carrasco, C. Frank, and C.N. Ta, Invest. Ophthalmol. Vis. Sci. **47:(E-Abstract 3592)**, (2006).
J.C. Barber, Int. Ophthalmol. Clin. **28**, 103–109 (1988).
H. Cardona, Refract. Corneal. Surg. **7**, 468–471 (1991).
D.J. Carlsson, F. Li, S. Shimmura, and M. Griffith, Curr. Opin. Ophthalmol. **14**, 192–197 (2003).
T.V. Chirila, Biomaterials **22**, 3311–3317 (2001).

G.M. Cruise, D.S. Scharp, and J.A. Hubbell, Biomaterials **19**, 1287–1294 (1998).
C. Czeslik, G. Jackler, T. Hazlett, E. Gratton, R. Steitz, A. Wittemann, and M. Ballauff, Physical Chemistry Chemical Physics **6**, 5557–5563 (2004).
M.G. Doane, C.H. Dohlman, and G. Bearse, Cornea **15**, 179–184 (1996).
C. Gao, X. Hu, Y. Hong, J. Guan, and J. Shen, J. Biomater. Sci., Polym. Ed. **14**, 937–950 (2003).
J.P. Gong, Y. Katsuyama, T. Kurokawa, and Y. Osada, Adv. Mater. **15**, 1155–1158 (2003).
M. Griffith, M.A. Watsky, C.Y. Liu, and V.T. Randall, In: A. Atala and R.P. Lanza (Eds.), *Epithelial Cell Culture: Cornea, in Methods of Tissue Engineering* (Academic Press, San Francisco, 2002) pp. 131–140.
J. Guan, C. Gao, F. Linxian, and J. Sheng, J. Biomater. Sci., Polym. Ed. **11**, 523–536 (2000).
A. Halperin, Langmuir **15**, 2525–2533 (1999).
C.R. Hicks, T.V. Chirila, P.D. Dalton, A.B. Clayton, S. Vijayasekaran, G.J. Crawford, and I.J. Constable, Aust. N Z J Ophthalmol. **24**, 297–303 (1996).
C.R. Hicks, G.J. Crawford, D.T. Tan, G.R. Snibson, G.L. Sutton, N. Downie, T.D. Gondhowiardjo, D.S. Lam, L. Werner, D. Apple, and I.J. Constable, Cornea **22**, 583–590 (2003).
C.R. Hicks, J.H. Fitton, T.V. Chirila, G.J. Crawford, and I.J. Constable, Surv. Ophthalmol. **42**, 175–189 (1997a).
C.R. Hicks, X. Lou, S. Platten, A.B. Clayton, S. Vijayasekaran, H.J. Fitton, T.V. Chirila, G.J. Crawford, and I.J. Constable, Aust. N Z J Ophthalmol. **25**(Suppl 1), S50–2 (1997b).
C.R. Hicks, S. Vijayasekaran, T.V. Chirila, S.T. Platten, G.J. Crawford, and I.J. Constable, Cornea **17**, 301–308 (1998).
K. Hille, H. Landau, and K.W. Ruprecht, Ophthalmologe **99**, 90–95 (2002).
D.A. Hoeltzel, D. Altman, K. Buzard, and K. Choe, J. Biomechan. Engin. **114**, 202–215 (1992).
M.M. Ismail, J. Cataract Refract. Surg. **28**, 527–530 (2002).
B. Khan, E.J. Dudenhoefer, and C.H. Dohlman, Curr. Opin. Ophthalmol. **12**, 282–287 (2001).
F. Li, D. Carlsson, C. Lohmann, E. Suuronen, S. Vascotto, K. Kobuch, H. Sheardown, R. Munger, M. Nakamura, and M. Griffith, Proc. Natl. Acad. Sci. USA **100**, 15346–15351 (2003).
V.A. Liu and S.N. Bhatia, Biomed. Microdev. **4**, 257–266 (2002).
X. Lou and V. Coppenhagen., Polym. Intern. **50**, 319–325 (2001).
T. Matsuda, K. Inoue, and T. Sugawara, ASAIO Transactions **36**, M559–M562 (1990).
T. Matsuda and T. Sugawara, Langmuir **11**, 2272–2276 (1995).
V. Moser, D.C. Anthony, W.F. Sette, and R.C. MacPhail, Fund. Appl. Toxicol. **18**, 343–352 (1992).
D. Myung, W. Koh, J. Ko, J. Noolandi, M. Carrasco, A. Smith, C. Frank, and C. Ta, Invest. Ophthalmol. Vis. Sci. **46: E-Abstract 5003**, (2005).
Y. Nakayama and T. Matsuda, Langmuir **15**, 5560–5566 (1999).
I.S. Nash, P.R. Greene, and C.S. Foster, Exp. Eye. Res. **35**, 413–424 (1982).
K.T. Nguyen and J.L. West, Biomaterials **23**, 4307–4314 (2002).
M. Nouri, H. Terada, E.C. Alfonso, C.S. Foster, M.L. Durand, and C.H. Dohlman, Arch. Ophthalmol. **119**, 484–489 (2001).
O. Olabisi, L.M. Robeson, and M.T. Shaw, Polymer-Polymer Miscibility (Academic Press, New York, 1979).
N.C. Padmavathi and P.R. Chatterji, Macromolecules **29**, 1976–1979 (1996).
S. Pintucci, F. Pintucci, S. Caiazza, and M. Cecconi, Eur. J. Ophthalmol. **6**, 125–130 (1996).
C.P. Quinn, C.P. Pathak, A. Heller, and J.A. Hubbell, Biomaterials **16**, 389–396 (1995).
H. Saito, A. Sakurai, M. Sakakibara, and H. Saga, J. Appl. Polym. Sci. **90**, 3020–3025 (2003).
B. Strampelli, Ber. Zusammenkunft. Dtsch. Ophthalmol. Ges. **71**, 322–335 (1972).
D.F. Sweeney, R.Z. Xie, M.D. Evans, A. Vannas, S.D. Tout, H.J. Griesser, G. Johnson, and J.G. Steele, Invest. Ophthalmol. Vis. Sci. **44**, 3301–3309 (2003).
V. Trinkaus-Randall, J. Capecchi, L. Sammon, D. Gibbons, H.M. Leibowitz, and C. Franzblau, Invest. Ophthalmol. Vis. Sci. **31**, 1321–1326 (1990a).
V. Trinkaus-Randall, A.W. Newton, and C. Franzblau, Invest. Ophthalmol. Vis. Sci. **31**, 440–447 (1990b).
V.L. Tsang, and S.N. Bhatia, Adv. Drug. Deliv. Rev. **56**, 1635–1647 (2004).
A.G. Tsuk, V. Trinkaus-Randall, and H.M. Leibowitz, J. Biomed. Mater. Res. **34**, 299–304 (1997).
S. Vijayasekaran, T.V. Chirila, T.A. Robertson, X. Lou, J.H. Fitton, C.R. Hicks, and I.J. Constable, J. Biomater. Sci. Polym. Ed. **11**, 599–615 (2000).
A. Wittemann, B. Haupt, and M. Ballauff, Phys. Chem. Chem. Phys. **5**, 1671–1677 (2003).